Applied Acoustics **41** (1994) 81–91

Technical Note

Acoustical Mechanisms and Performance of Various Active Duct Noise Control Systems

Sen M. Kuo & Jianming Tsai

Department of Electrical Engineering, Northern Illinois University, DeKalb, Illinois 60115, USA

(Received 18 November 1992; accepted 26 November 1992)

ABSTRACT

Based on the analysis of the characteristics of sound wave propagation in a duct, three Active Noise Control (ANC) systems, which incorporate different arrangements of the secondary loudspeaker have been examined experimentally. Calculated and measured transfer functions of the plant and the error paths show good agreement in the acoustic modal frequencies of the systems. Real-time tests show a more effective noise attenuation with tree-shaped configuration than with the traditional T-shaped ANC system. The symmetric arrangement of two secondary speakers in the tree-shaped system helps in compensating the node observed at 200 Hz in the error path. This compensation can be also achieved by using an equalizer.

1 INTRODUCTION

Active noise control technique, which uses a secondary sound to destructively interfere with the primary noise, thus reducing the level of noise in an economical way, has been employed. A basic active noise control system for cancelling the duct noise consists of a detector sensor, a secondary actuator, and an error sensor. The detected signal is fed through the control filters to generate a signal which drives the secondary actuator. The coefficients of the control filters are adjusted to obtain a

Applied Acoustics 0003-682X/93/$06.00
Printed in Great Britain

minimized signal at the error sensor position. Much of the theoretical and experimental work has been carried out in the area of active control of noise in waveguides. But the existence of acoustic nodes in the error path leads to difficulties in using active noise control systems effectively. The influence of the reflections from the duct terminations and the discontinuities, on the effectiveness of a random noise attenuation has been discussed by Fontaine and Shepherd.[1]

Three active noise control systems which incorporate different arrangements of the secondary speaker have been designed and tested. Figure 1 shows the configuration of these systems, wherein the source speaker was situated at the left end, the secondary speaker(s) at the branch, the detection sensor was located very close to the primary source, and the error sensor was put at the right end (i.e. the output end). The actual dimensions of these three systems are listed in Table 1.

The T-shaped configuration is known as a traditional ANC system. In this arrangement, the upstream reflections are large, and this would affect the performance and the stability of the system. The acoustic feedback

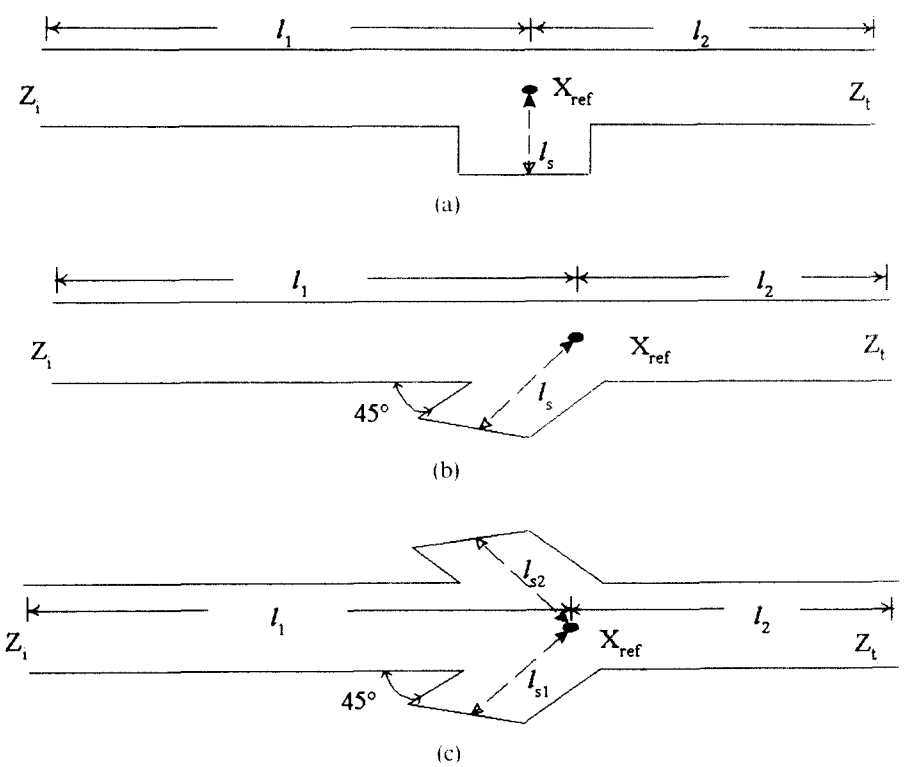

Fig. 1. Schematic diagram of three active noise control systems; (a) T-shaped system, (b) half-Y-shaped system, (c) tree-shaped system.

TABLE 1
Dimensions of Three ANC Systems

ANC systems	l_1 (*cm*)	l_2 (*cm*)	l_{s1} (*cm*)	l_{s2} (*cm*)	*Radius a* (*cm*)
T-shaped	40·64 (16·0 in)	34·29 (13·5 in)	11·43 (4·5 in)	—	7·62
Y-shaped	44·45 (17·5 in)	34·29 (13·5 in)	7·62 (3·0 in)	—	7·62
Tree-shaped	44·45 (17·5 in)	34·29 (13·5 in)	7·62 (3·0 in)	7·62	7·62

from the secondary source contaminates the reference signal received by the detector sensor and also forms an infinite feedback loop in the system. Therefore, the Y-shaped and tree-shaped systems were designed to have the secondary speakers at 45° angles to the main duct.

The transfer functions of the plant and the error paths have been calculated using the acoustic transmission line theory, and the calculated modal frequencies show good agreement with the measured ones. This paper will focus on the discussion of the noise attenuation with different arrangements of secondary source.

2 ACOUSTICAL CONSIDERATIONS OF ANC SYSTEMS

We use a model of matching plane waves coupled with the Kirchhoff theory of viscothermal losses in tubes. This approach allows representation of a duct as a transmission line for plane waves.[2] Because the model is one unidimensional, the sound pressure P and volume velocity U must be considered as averages over the cross-section of the duct. The element linking the input (P_{in}, U_{in}) to the output (P_{out}, U_{out}) can be described by a 2×2 matrix:

$$\begin{bmatrix} P_{in} \\ U_{in} \end{bmatrix} = \begin{bmatrix} A & B \\ C & D \end{bmatrix} \begin{bmatrix} P_{out} \\ U_{out} \end{bmatrix} \tag{1}$$

From this general equation, the transfer function P_{out}/P_{in}, the input impedance P_{in}/U_{in}, or the transfer impedance P_{out}/U_{in} can be calculated. Our approach was to perform calculations of transfer impedance in various ANC systems. Although the detailed derivation is not addressed here, however, the expression of transfer impedance can be written as

$$Z_{tr} = \frac{Z_t U_{out}}{CP_{out} + DU_{out}} = \frac{Z_t}{CZ_t + D} \tag{2}$$

where Z_t is the termination impedance, $Z_t = P_{out}/U_{out}$, C and D are

elements in the resultant *ABCD* matrix. For a finite, lossless acoustic transmission line, the *ABCD* matrix is expressed as[3]

$$\begin{bmatrix} A & B \\ C & D \end{bmatrix} = \begin{bmatrix} \cos kl & \mathrm{j}R_0 \sin kl \\ (1/R_0) \sin kl & \cos kl \end{bmatrix} \tag{3}$$

where $R_0 = \rho c/S$ is the characteristic impedance of the duct, ρ is the density of the air, c is the speed of sound, S is the cross-sectional area of the duct, k is the wave vector, and l is the total length of the duct.

Usually, a complicated duct system is regarded as a series of elemental geometric shapes. Then the resultant matrix $\mathbf{A}_{res}$ of a system with n elements is the product of the individual matrices from the input to the output end, which is

$$\mathbf{A}_{res} = \begin{bmatrix} A & B \\ C & D \end{bmatrix} = \begin{bmatrix} A_1 & B_1 \\ C_1 & D_1 \end{bmatrix} \begin{bmatrix} A_2 & B_2 \\ C_2 & D_2 \end{bmatrix} \cdots \begin{bmatrix} A_n & B_n \\ C_n & D_n \end{bmatrix} \tag{4}$$

For example, a shunt element, such as a side branch in a duct, is analogous to a parallel circuit. Assuming Z_s to be the impedance of the branch, the matrix for the shunt is[3]

$$\begin{bmatrix} A & B \\ C & D \end{bmatrix} = \begin{bmatrix} 1 & 0 \\ 1/Z_s & 1 \end{bmatrix} \tag{5}$$

In reality the sound wave cannot transverse a pipe without losing at least a small amount of energy, either due to absorption in the walls of a duct or due to viscous friction impeding the air nearest the wall. Then the wave vector k becomes a complex number $k' = \alpha + \mathrm{j}k$, where α is the total effective damping constant considering viscothermal loss near the duct wall as given by Keefe.[4] Since the output end of the ANC system opens to free space, we chose the radiation impedance as the termination impedance. The radiation impedance is expressed as

$$Z_t = R_0 \left[1 - \frac{J_1(2k'a)}{k'a} + \mathrm{j} \frac{K_1(2k'a)}{2(k'a)^2} \right] \tag{6}$$

where J_1 and K_1 are two types of Bessel functions, and a is the radius of the duct.

In an ANC system, the plant path is defined as the path from the source speaker to the error microphone, whereas the term error path signifies the path from the secondary speaker to the error microphone. The frequency responses of the transfer impedances can be calculated using eqns (2) and (6), where *A*, *B*, *C* and *D* are the resultant matrix values under consideration of system construction. The frequency responses of the plant and error paths for three ANC systems are shown using dashed lines in Figs 3–5.

3 REAL-TIME EXPERIMENTS AND ANALYSIS

3.1 Measurements of transfer functions

As mentioned above, in an ANC system, we usually use several transfer functions to describe the system. For instance, $P(z)$ is the transfer function of the plant path and $He(z)$ is that of the error path. The experimental setup for an ANC system is shown in Fig. 2. The plant and the error paths for each system are off-line modeled by using a HP3563A two-channel FFT analyzer and the frequency responses are plotted using solid lines in Figs 3–5. Comparison of the curves shows very good agreement in the calculated and the measured values of the modal frequencies of the plant and the error paths transfer functions. But in Fig. 5(b), the measured error path does not show a node at 200 Hz, unlike the calculated curve. This will be analyzed later.

3.2 Measurements of noise reduction

Real-time experiments were carried out in order to make a comparison of the amount of noise reduction achieved by the three different systems as shown in Fig. 1. The filtered-X LMS algorithm was used and implemented on a DSP56001 signal processor for active noise control. Figure 6 gives the block diagram of this algorithm. The test results are shown in Fig. 7, wherein the upper curve in each sub-graph is without using ANC, while the lower one with ANC.

The T-shaped and the Y-shaped arrangements result in a similar amount of noise reduction over the desired frequency range, but the tree-shaped system shows a very promising improvement at the dead point of the T-shaped system. This could be explained as the compensation of the node at 200 Hz in the error path due to the symmetric arrangement of

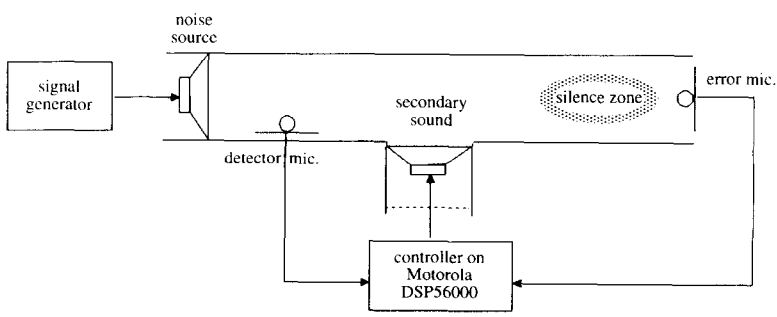

Fig. 2. The experimental setup for an active noise control system.

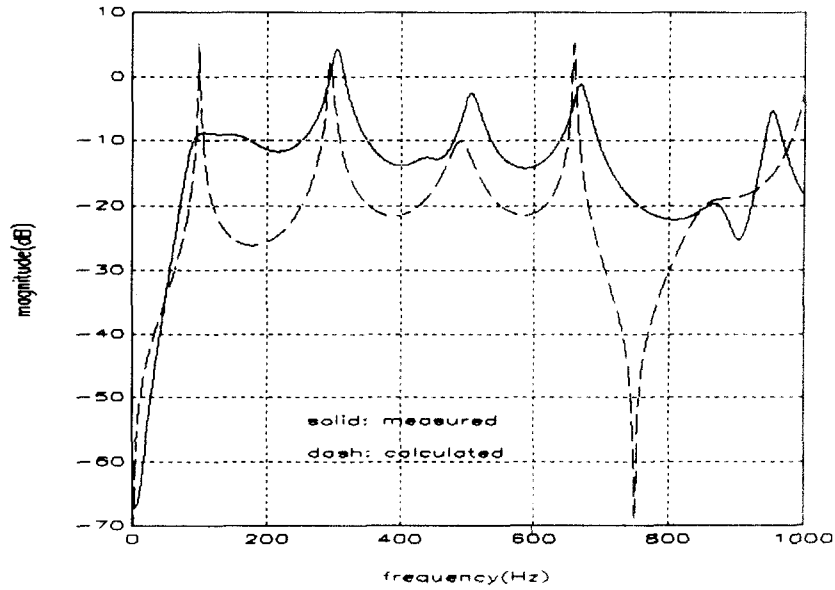

(a)

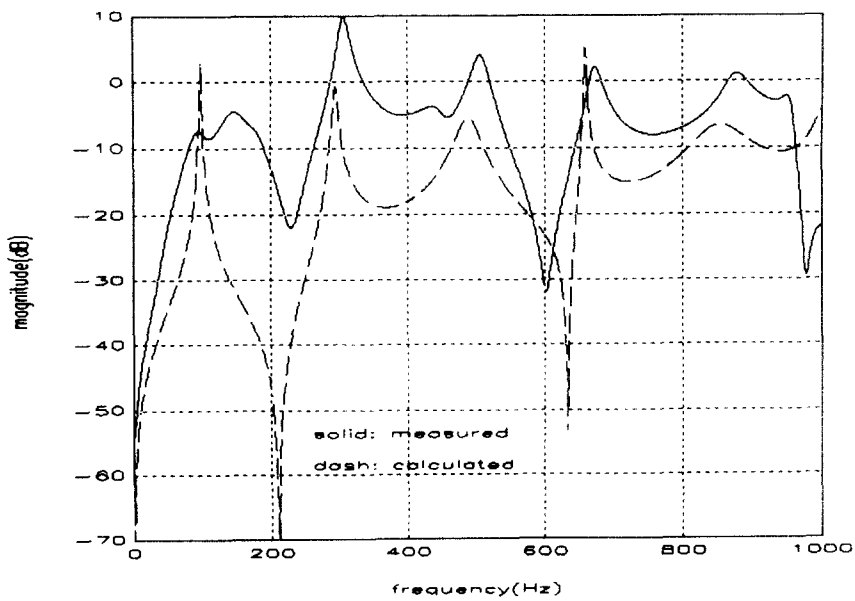

(b)

Fig. 3. Measured and calculated frequency responses of T-shaped ANC system; (a) plant path, (b) error path.

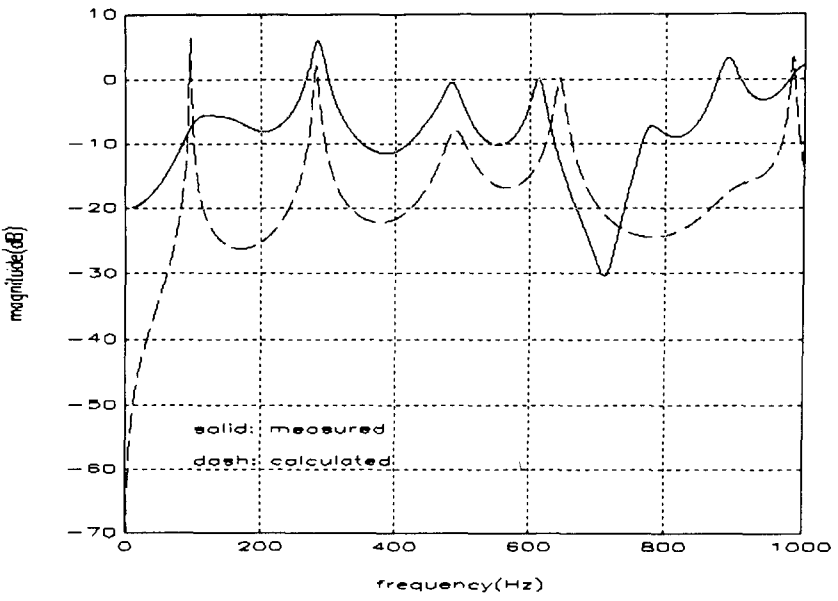

(a)

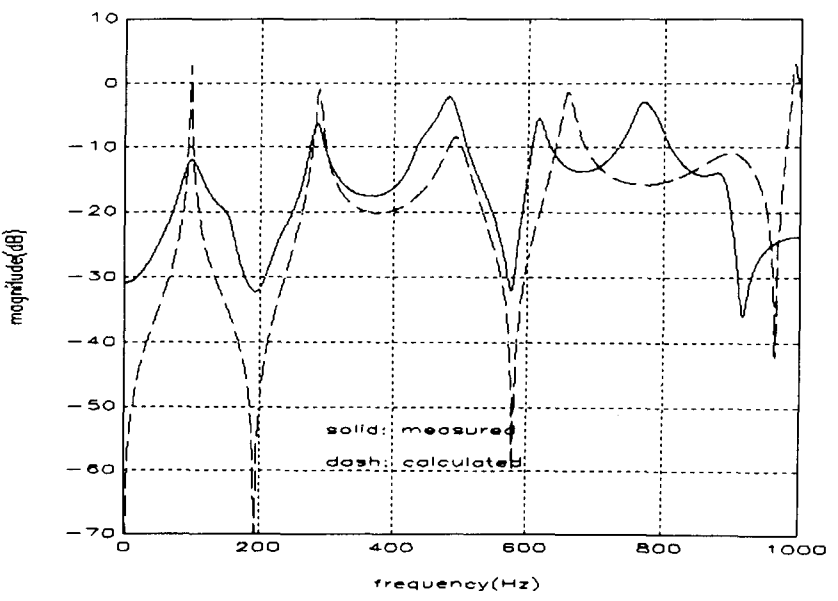

(b)

Fig. 4. Measured and calculated frequency responses of Y-shaped ANC system; (a) plant path, (b) error path.

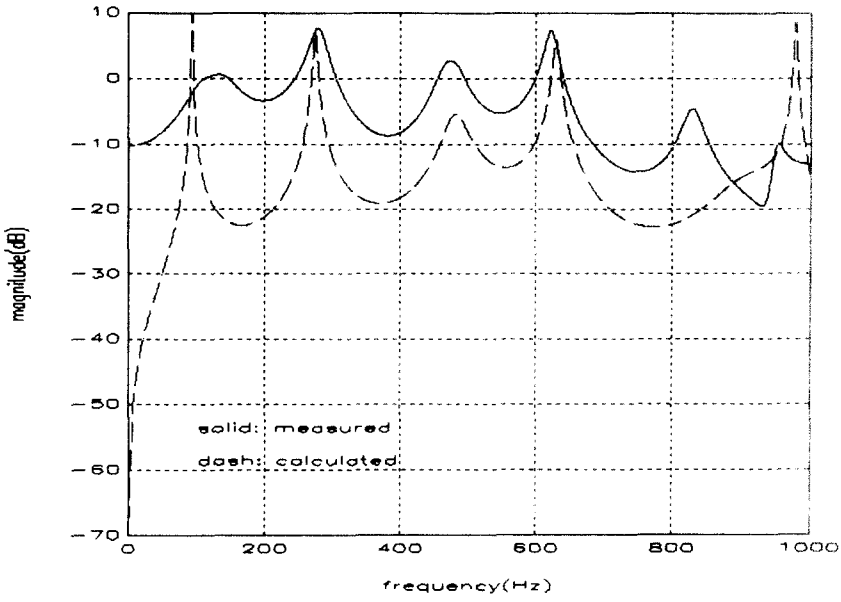

(a)

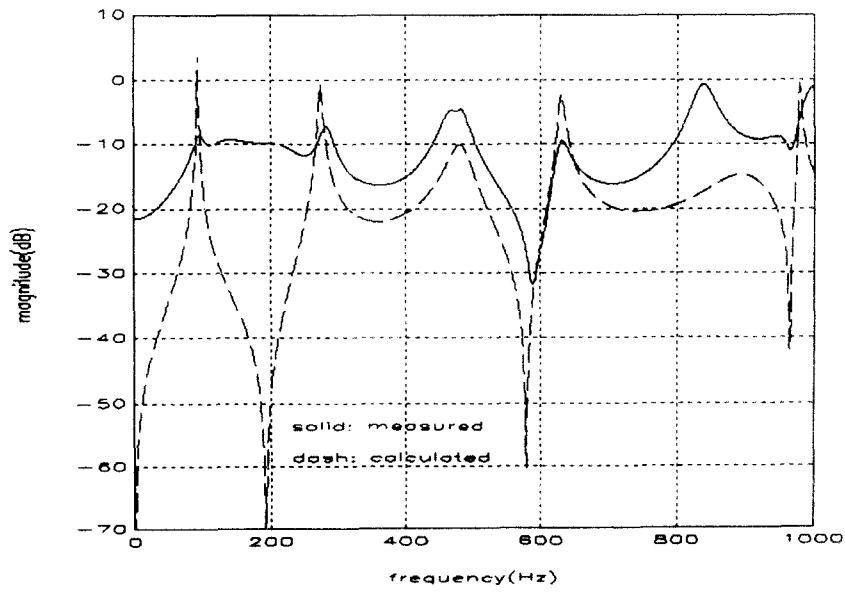

(b)

Fig. 5. Measured and calculated frequency responses of tree-shaped ANC system; (a) plant path, (b) error path.

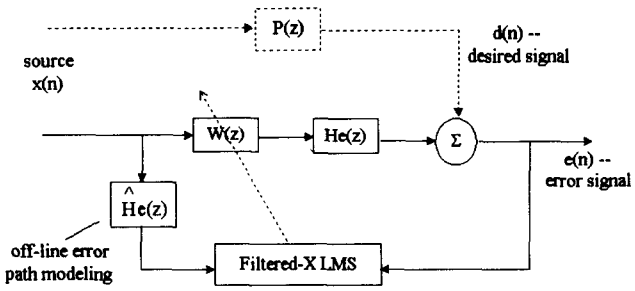

Fig. 6. The filtered-X LMS algorithm for real-time active noise control.

the secondary speakers (referring to Figs 4(b) and 5(b)). At certain frequencies which correspond to resonant conditions, the effects of the evanescent modes become significant even when the mode is not close to its cut-on frequency, such as 200 Hz. When the driving frequency approaches this mode, the evanescent wave is relatively strong, and less attenuated with distance, since the error microphone was located close to the side branch, within a quarter of the wavelength at 200 Hz. As a result, the error microphone detects the evanescent wave at the discontinuity, and the symmetry of the secondary speakers helps in improving noise cancellation at this frequency.

3.3 Inverse modeling

From the above analysis, the performance of an ANC system depends largely upon the transfer function of the error path. If there exists a node in the error path, a very small amount of signal will be detected by the error microphone at this frequency. As a consequence, the control part would not adjust the filter coefficients properly, resulting in small or no cancellation at this frequency. By introducing an equalizer in the system, the error path can be modulated before feeding back into the control unit. For a Y-shaped ANC system, we can achieve the effect of tree-shaped system without using another secondary source. The noise reduction is increased by about 10 dB in the frequency range from 100 Hz to 250 Hz (see Fig. 8a), which corresponds to the amount of compensation in the error path by using the equalizer (see Fig. 8b).

On the basis of these experimental measurements and analysis, it is possible to provide a primary diagnostic for any ANC system using acoustic transmission line theory, and then apply an equalizer or symmetric arrangement of secondary source to improve the performance. Further studies could be proposed by using digital equalization to obtain effective noise cancellation over the desired frequency range.

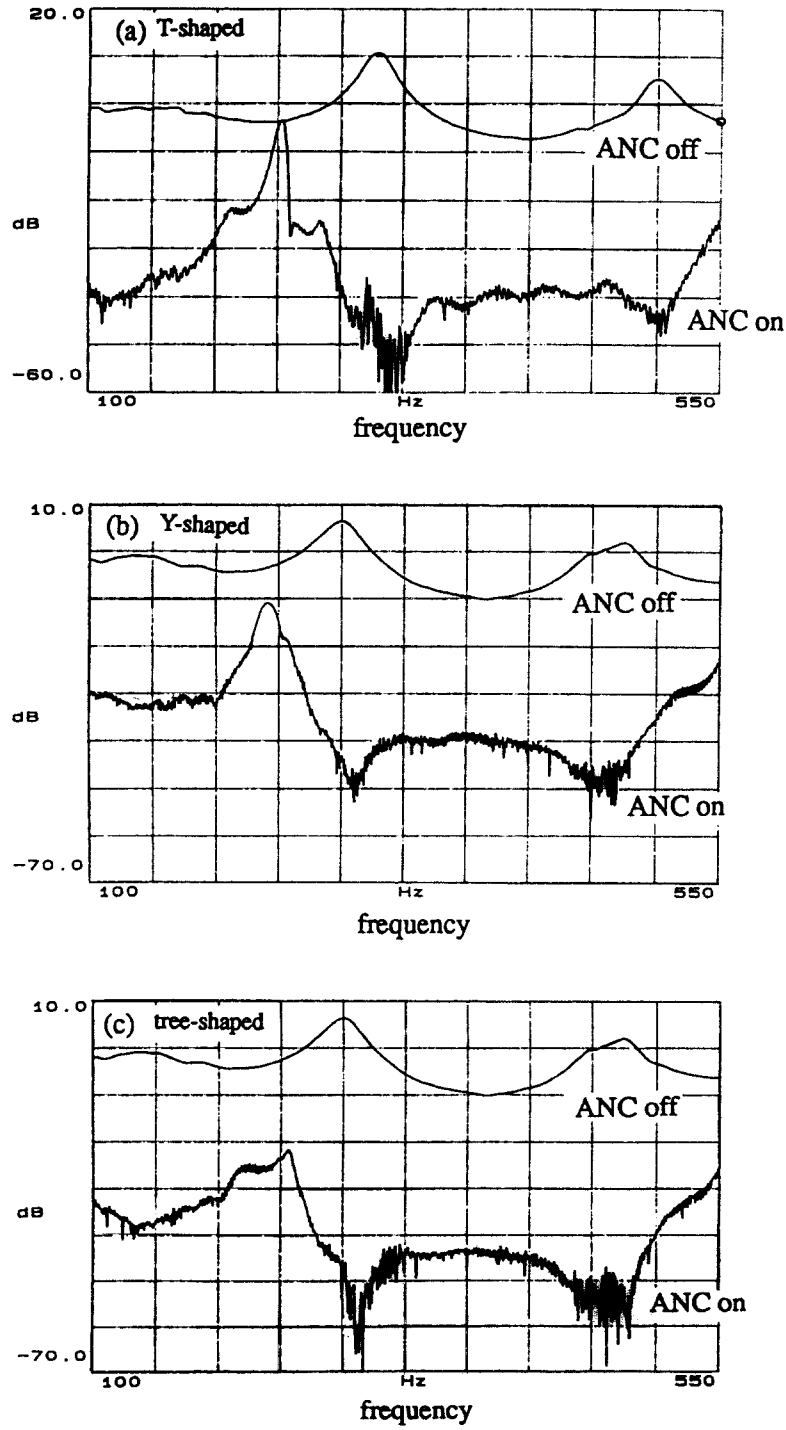

Fig. 7. Noise reduction of three ANC systems.

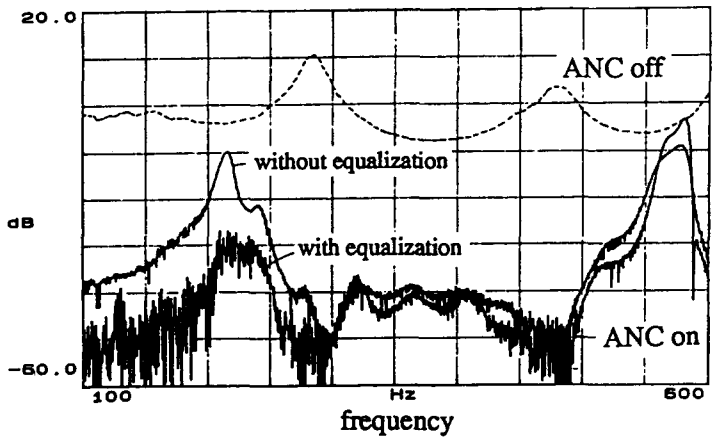

Fig. 8a. Noise attenuation with and without equalizer for Y-shaped ANC system.

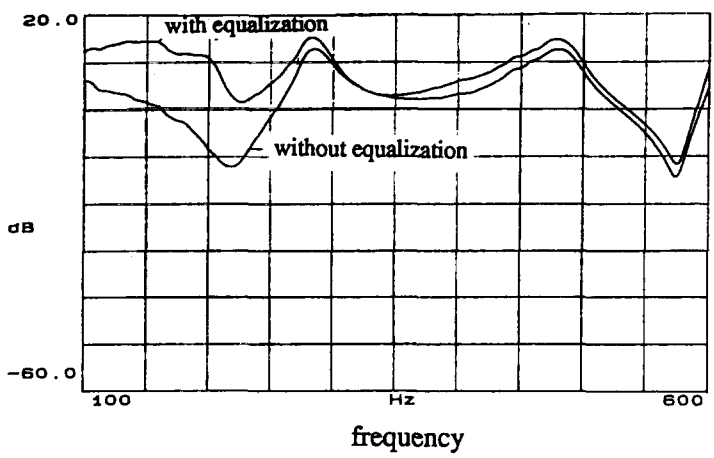

Fig. 8b. Frequencies responses of modified and original error path for Y-shaped ANC system.

REFERENCES

1. La Fontaine, R. F. & Shepherd, I. C., The influence of waveguide reflections and system configuration on the performance of an active noise attenuator. *J. Sound Vib.*, **100**(4) (1985) 569–79.
2. Causse, R., Input impedance of brass musical instruments—comparison between experiment and numerical models. *J. Acoust. Soc. Amer.*, **75**(1) (1984) 241–53.
3. Hoekje, P., Lecture notes from graduate course on Acoustics II, Spring, 1991.
4. Keefe, D. H., Acoustical wave propagation in cylindrical ducts. *J. Acoust. Soc. Amer.*, **75**(1) (1984) 58–62.